Electronic Supporting Information

A New Class of Soluble and Stable Transition-Metal-Substituted Polyoxoniobates: [Cr$_2$(OH)$_4$Nb$_{10}$O$_{30}$]$^{8-}$.

Jung-Ho Son, C. André Ohlin and William H. Casey*

A) Computational Results

The two most interesting aspects of this new polyoxoanion is the inclusion of a more redox active metal and the optical activity in the visible region. For these reasons we in particular wanted to explore whether it was possible to readily and routinely predict the location of the absorbance bands of this type of compound. Also, owing to the difficulty in isolating the oxidised and reduced forms of the central polyanion dichromate species, we employed computations at the density functional theory (DFT) level to get a better idea of the potential characteristics of these forms. Structures were optimised for anti-parallel and parallel electronic spin alignments, and for both high and low spin cases where relevant. Intermediate spin configurations were also tested for [Cr$_2$(OH)$_4$Nb$_{10}$O$_{30}$]$^{8-}$. As expected, the high spin form of the Cr^{II}Cr^{III} complex was favoured (Table S1, below).

DFT overestimates the bond lengths in general, but gives a good picture of the general distortion of the octahedral chromium unit, and in agreement with the crystal structure predicts that the shortest bond is the Cr-μ_2-O bond *trans* from the central μ_6-oxygen in the Lindqvist unit, and that the (Nb-)μ_2-O-Cr-μ_4-O(-Nb,Nb,Cr) angle is smaller by *ca* 5° from the ideal 180°. The predictive power is surprisingly good even when using 3-21G/3-21G* and b3lyp when taking into account the limitations inherent in implicit solvent models which do not account for specific interactions such as hydrogen bonding, which are likely to be important in water. The counterions were also excluded from the computations, which are reasonable approaches if the Arrhenius model is strictly true; however, examples of polyoxometalates interacting strongly with their counterions in solution are well known.[1]

Electronic transitions were predicted to occur at 422 and 509 nm using LANL2DZ/ECP on Nb and Cr, and 6-31+G* on all other atoms, together with the conductor-like screening model (COSMO) and the b3lyp exchange and correlation functional in NWChem 6.1 (Table S2, entry 3, below).[2] While the positions of the bands were poorly predicted, the relative ratios of the intensities of the transitions agreed fairly well with the observed spectrum, in particular given the difficulties of modeling a system with such a high negative charge and delocalized electrons.

We found that NWChem using COSMO and the 3-21G (Nb,Cr) and 3-21G* (O,H) basis sets predicted the location of the electronic transition bands fairly well (Table S2, entry 5, below), at the cost of poor predictive power for the relative intensities. Gaussian 09 using PCM but otherwise identical parameters faired slightly worse (Table S2, entry 2, below).[3] Neither approach is perfect, but from the point of view of providing diagnostic data, 3-21G basis sets seem to be accurate enough for these systems, in accordance with the observations of Grätzel et al.[4]

We attempted to expand our study to include the electronic spectra of the reduced and oxidised analogues of the polyanion, but given the lack of reference spectra it is difficult to evaluate the reliability of this approach. Firstly, using NWChem we found that the 32 lowest energy transitions in the reduced species all occurred above 1200 nm, while Gaussian found transitions in the near IR region. Rather than focussing too much on the predicted bands, a more reasonably interpretation is that the number of empty *d*-orbitals of similar energies coupled with the large number of unpaired electrons will likely lead to strong absorbances over a wide range of wavelengths. Likewise, an attempt at modelling the absorbance spectrum of the hypothetical oxidised Cr^{IV}Cr^{III} polyoxometalate species suggested that the bands are bathochromically shifted.

The spectra were visualised by applying gaussian broadening functions to each transition scaled by the oscillatory strength of the transition, and plotting the cumulative sum of the contribution of each peak at each given wavelength (Figure 3 in article). There are more rigorous and accurate approaches to the computation of electronic spectra of polyoxometalates,[5] as well as better solvation models that account for both specific and non-specific interactions. However, ultimately the computational methods employed here were deliberately reduced to be as computationally cheap and conceptually simple as possible, as to evaluate whether DFT can be used to routinely predict and evaluate experimental electronic spectra data without requiring a costly investment in computational resources.

Table S1. Electronic energies of $[Cr^xCr^{III}(OH)_4Nb_{10}O_{30}]^{(11-x)-}$ (x=II,III,IV) using structures optimized by unrestricted DFT in Gaussian '09 using the LANL2DZ/ECP basis set for niobium and chromium, and the polarization and diffusion augmented 6-31+G* basis set on oxygens and protons. The optimization and energy calculations were carried out in the presence of a polarizable continuum model (PCM) for a dielectric constant of 78.3553.

Entry	Cr Oxidation states[a]	Multiplicity	ε_0 (Hartree)
1	II,III	2	-3299.66550657
2	II,III	6	-3299.78977790
3	II,III	8	-3299.82334079
4	III,III	1	-3299.43790545
5	III,III	3	-3299.55153408
6	III,III	5	-3299.62993195
7	III,III	7	-3299.76029119
10	IV,III	2	-3299.38922103
11	IV,III	6	-3299.52371212

[a] The formal oxidation states for all other atoms were +5 (Nb) , -2 (O) and +1 (H).

Table S2. Major transitions of $[Cr^xCr^{III}(OH)_4Nb_{10}O_{30}]^{(11-x)-}$ (x=II,III,IV) in the visible region as calculated using Gaussian '09 and NWChem. Unless otherwise noted the 3-21G basis set was used on Cr and Nb, while the polarization augmented 3-21G* set was used for O and H. The b3lyp exchange and correlation functional was used in conjunction with the polarizable continuum model (G09) or the conductor-like screening model (NWChem) as implemented for water in either package.

Entry	Cr Oxidation states[a]	λ (nm)
1[a,b]	II,III	662, 731, 774, 893, 1009
2[b]	III,III	434, 527
3[c,d]	III,III	422,509
4[d,e]	III,III	457,591
5[d]	III,III	448, 546
6[a,b]	IV,III	660, 726, 788
7[a,d]	IV,III	669, 773, 835

[a]Only transitions above λ = 650 nm and below 1100 nm have been included. [b]Gaussian 09. [c]The basis sets were LANL2DZ/ECP on Nb and Cr, and 6-31+G* on all other atoms. [d]NWChem 6.1. [e]Using the cam-b3lyp hybrid exchange and correlation functional.

B) Detailed experimental parameters

X-ray crystallography

Selected single crystals were coated with Paratone oil and mounted on a glass fibre tip. The diffraction data for **1** and **2** were collected on a Bruker Apex II diffractometer equipped with a Mo Kα source (λ = 0.71073Å) and the data for **3** was collected using a Bruker SMART 1000 diffractometer. Multi-scan absorption correction was applied with the SADABS program.[6] The structure was solved by using the SHELXTL program[7] with Patterson method (heavy atom method), which distinguished niobium and chromium sites. Further cycles of full-matrix least square refinement based on F^2 were carried out by SHELXL-97 program where most of the other atoms were located. Protons on the tetramethyl ammonium ions were fixed by the riding model. Protons on the cluster and crystallization water could be found in the difference Fourier map at the end of the refinement. Extinction correction was applied for the structures of **1** and **2**.

*Instrumental characterizations*

ESI-MS data were obtained on an Agilent G1958b single quadrupole spectrometer equipped with a syringe pump for direct source injection, with a cone voltage of -20 V and an injection rate of 30 μL/min. Infrared spectra were obtained on a Bruker Tensor 27 FT-IR spectrometer with KBr pellets dispersed with samples. A Varian Cary 300 UV-visible spectrometer was used for measuring the UV-vis absorption spectra. 40 mg of **3** was dissolved in 3 mL of water for measurement (12.6 mM based on Cr). For comparison, 10 mg of $CrCl_3 \cdot 6H_2O$ was dissolved in 3 mL of water (12.5 mM) and the spectra were measured separately. The cyclovoltammetry was carried out using a potentiostat/galvanostat model 263A (Princeton Applied Research). A conventional three-electrode cell was used for measurement with glassy carbon electrode (working), platinum wire (counter) and Ag/AgCl electrode (reference). Powder XRD was performed with a Bruker AXS D8 Advance diffractometer equipped with a Cu Kα radiation source (λ = 1.54056 Å) in the range of $2\theta = 5$–50° with 0.02° step size and 0.3 s per step.

Computational methods

Geometry optimisations and time-dependent density functional theory calculations were carried out using NWChem 6.1 and Gaussian 09 by unrestricted DFT calculations at the 3-21G (Nb,Cr)/3-21G*(O,H) and LANL2DZ(Nb,Cr)/6-31+G* (O,H) levels with the b3lyp correlation and exchange hybrid functional. The polarisable continuum model (PCM) and the conductor-like screening model was used to approximate the solvation in water in Gaussian 09 and NWChem, respectively. The range-separated CAM-b3lyp functional was implemented as described in the NWChem documentation. Time-dependent DFT calculations in NWChem were carried out using the CI singles approach, and by freezing the lowest 200 α and β orbitals. The computational approach was kept deliberately simple owing to the large number of transition metals in the cluster, and the goal was to achieve a functional model.

Table S3. Crystallographic parameters of **1-3**

	1	2	3
Empirical formula	$C_{40}H_{168}Cl_2Cr_2N_{10}Nb_{10}O_{56}$	$C_{12}H_{52}CrKN_3Nb_5O_{24}$	$H_{28}Cr_2K_8Nb_{10}O_{46}$
Formula weight	2789.84	1178.22	2110.12
T (K)	90(2)	90(2)	95(2)
Crystal system	Triclinic	Triclinic	Triclinic
Space group	P-1	P-1	P-1
Color/Shape	Green/Prism	Green/Hexagonal Prism	Green/Prism
a (Å)	11.9543(5)	10.8567(4)	9.6658(8)
b (Å)	12.7933(6)	14.0359(5)	10.6352(9)
c (Å)	17.4275(8)	14.0490(5)	11.4163(10)
a (deg)	76.505(1)	114.092(1)	75.245(1)
b (deg)	86.802(1)	100.702(1)	80.560(1)
g (deg)	73.545(1)	102.282(1)	87.655(1)
V (Å^3)	2485.39(19)	1818.30(11)	1119.50(16)
Z	1	2	1
ρ_{calcd} (g cm^{-3})	1.864	2.152	3.130
μ (mm^{-1})	1.464	2.012	3.785
Crystal size (mm)	0.29 x 0.29 x 0.23	0.18 x 0.11 x 0.11	0.20 x 0.19 x 0.15
θ range (deg)	2.30 to 27.50	2.63 to 30.55	2.91 to 27.62
Data / restraints / parameters	11387 / 0 / 658	11031 / 0 / 492	5072 / 0 / 354
GOF on F^2	1.053	1.166	1.083
R1/wR2 [I>2sigma(I)]	0.0205/0.0523	0.0235/0.0558	0.0238/0.0697
R1/wR2 (all data)	0.0243/0.0540	0.0275/0.0570	0.0271/0.0719
Extinction coefficient	0.00042(8)	0.00016(6)	
Largest diff. peak/hole (e·Å^{-3})	0.656 / -0.795	0.740 / -0.551	0.835 / -1.059
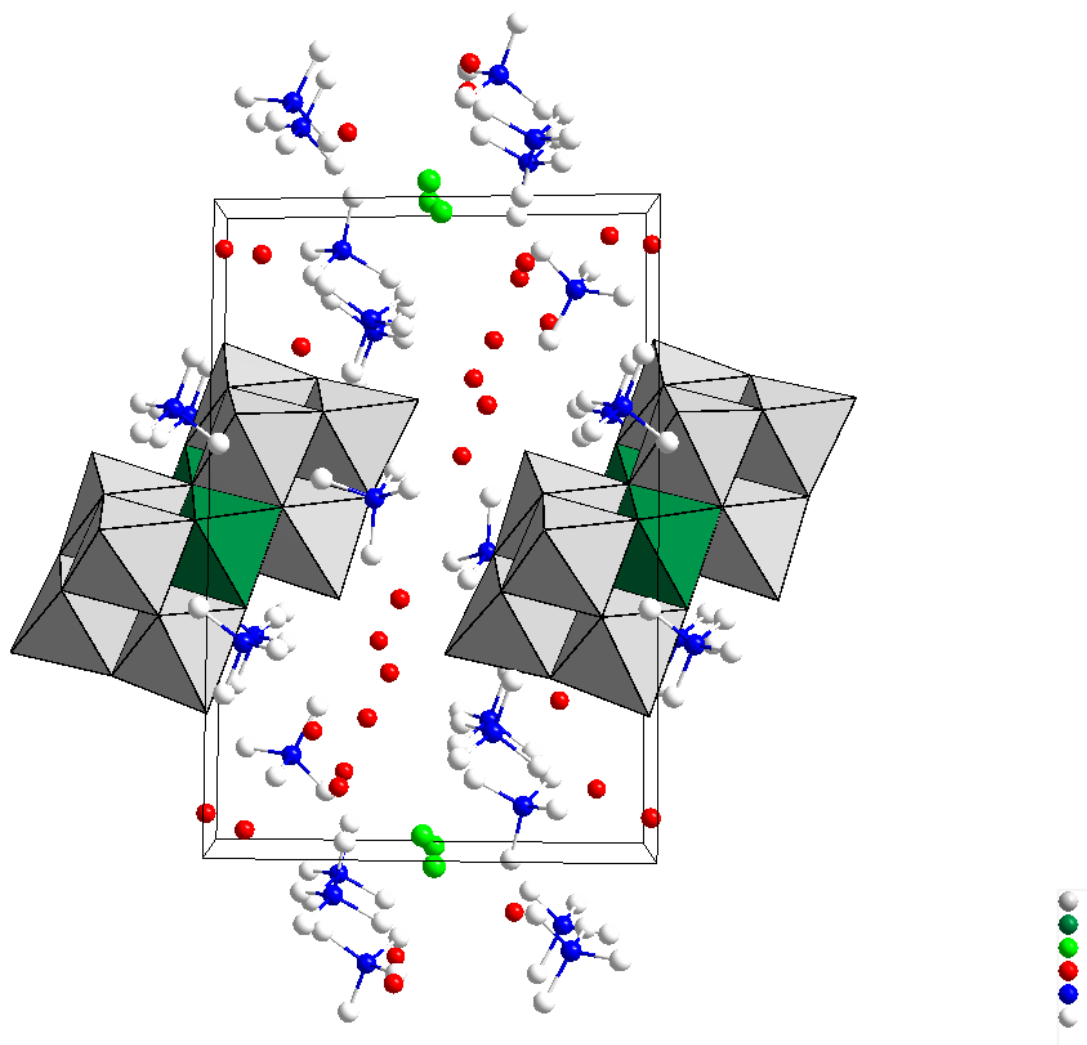
Figure S1. Unit cell content of **1** seen along the b axis (Grey: Nb, Green: Cr, Light Green: Cl, Red: O, Blue: N, White: C) .
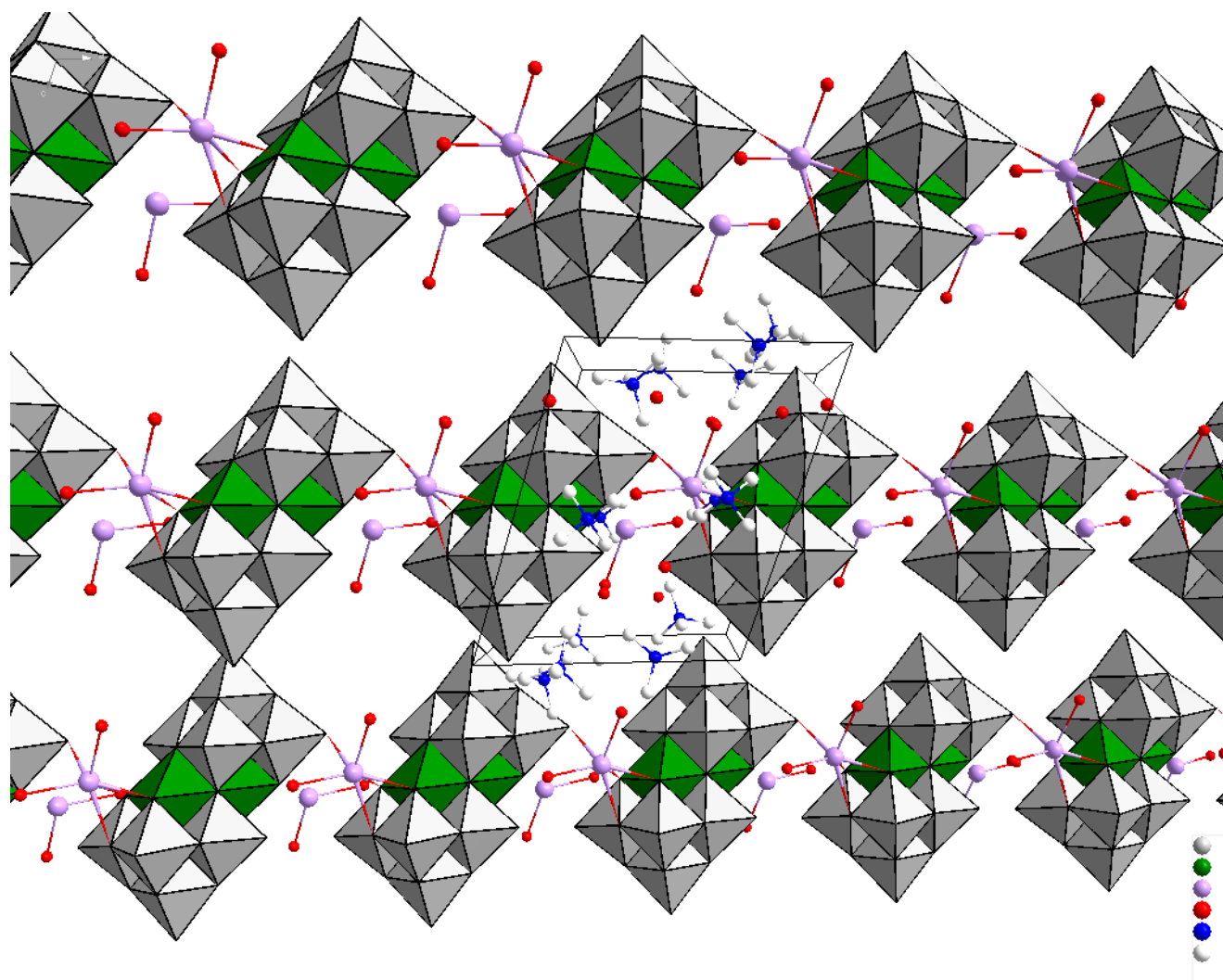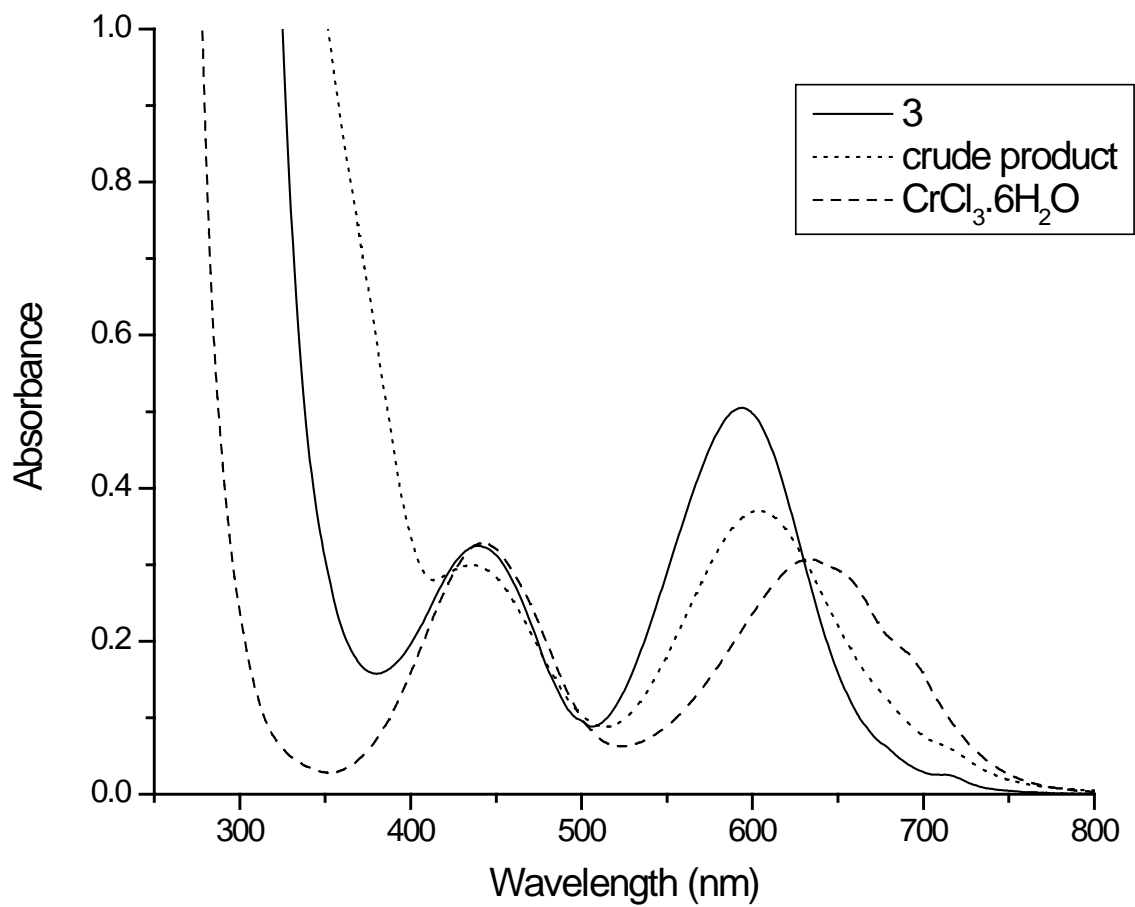
Figure S2. Unit cell content of **2** seen along the b axis (Grey: Nb, Green: Cr, Violet: K, Red: O, Blue: N, White: C).
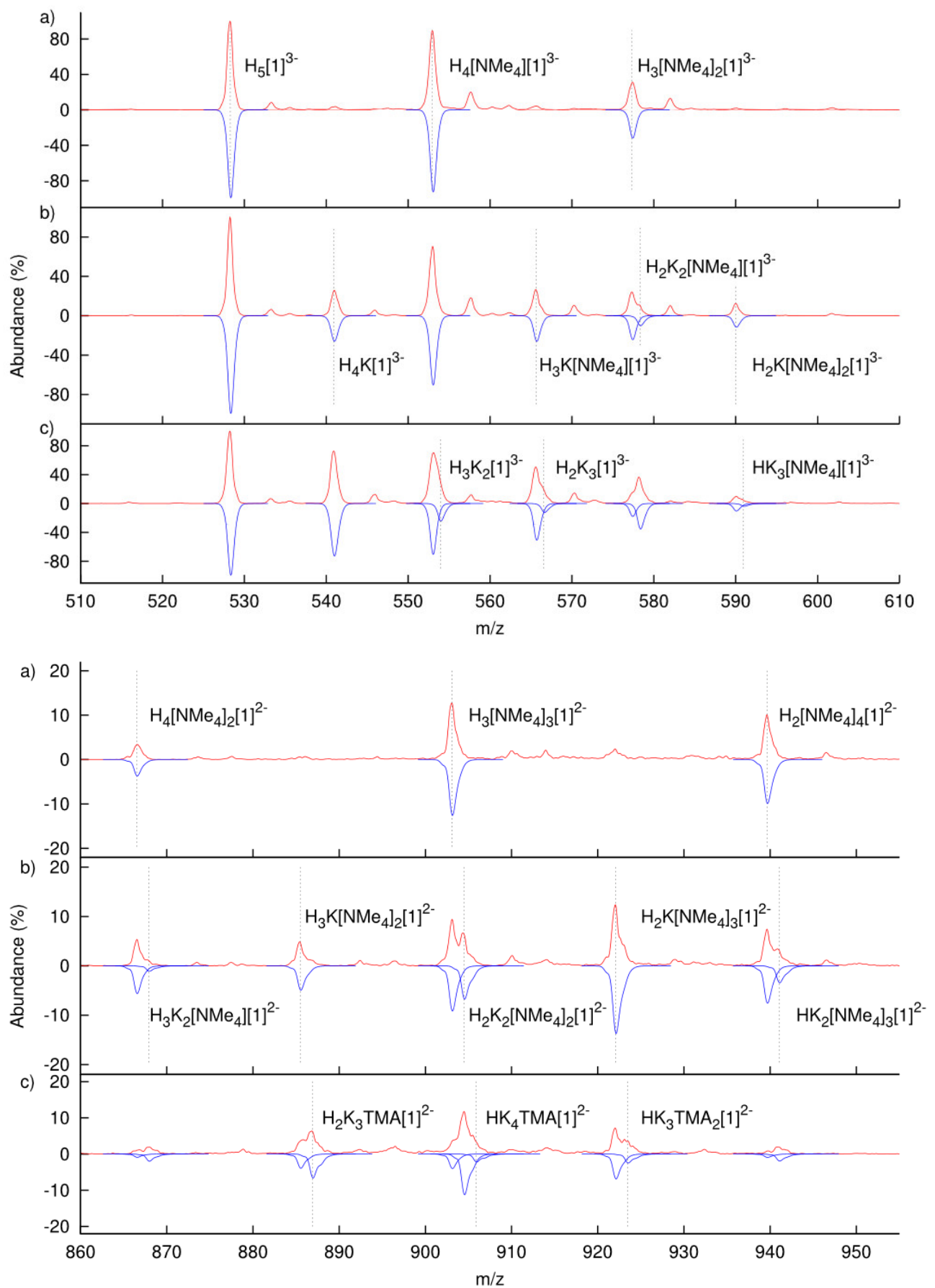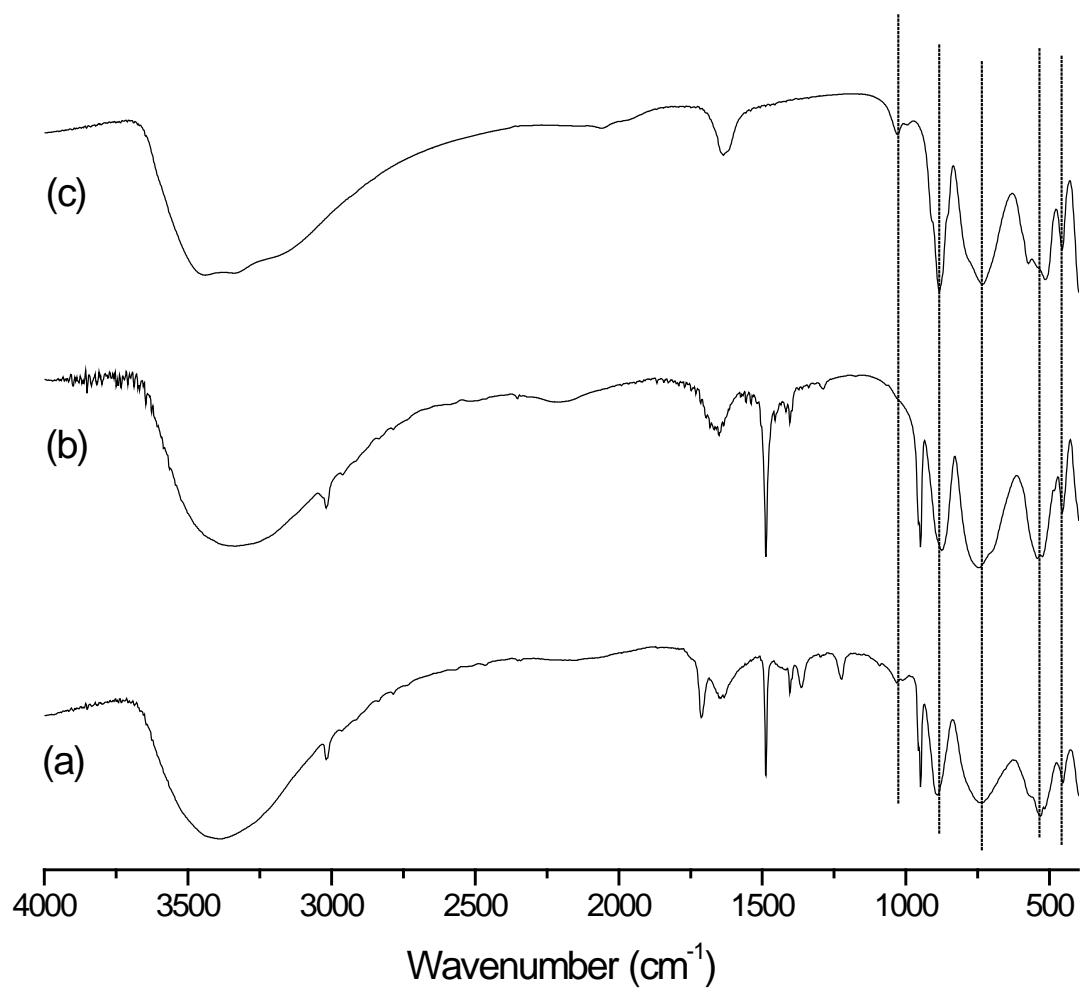
Figure S3. ESI-MS (red) and simulated MS peaks (blue) of a) **1**, b) **2**, and c) **3** in the 510-610 m/z region (upper) and 860-960 m/z region (lower). [1] stands for $[Cr_2(OH)_4Nb_{10}O_{30}]$.
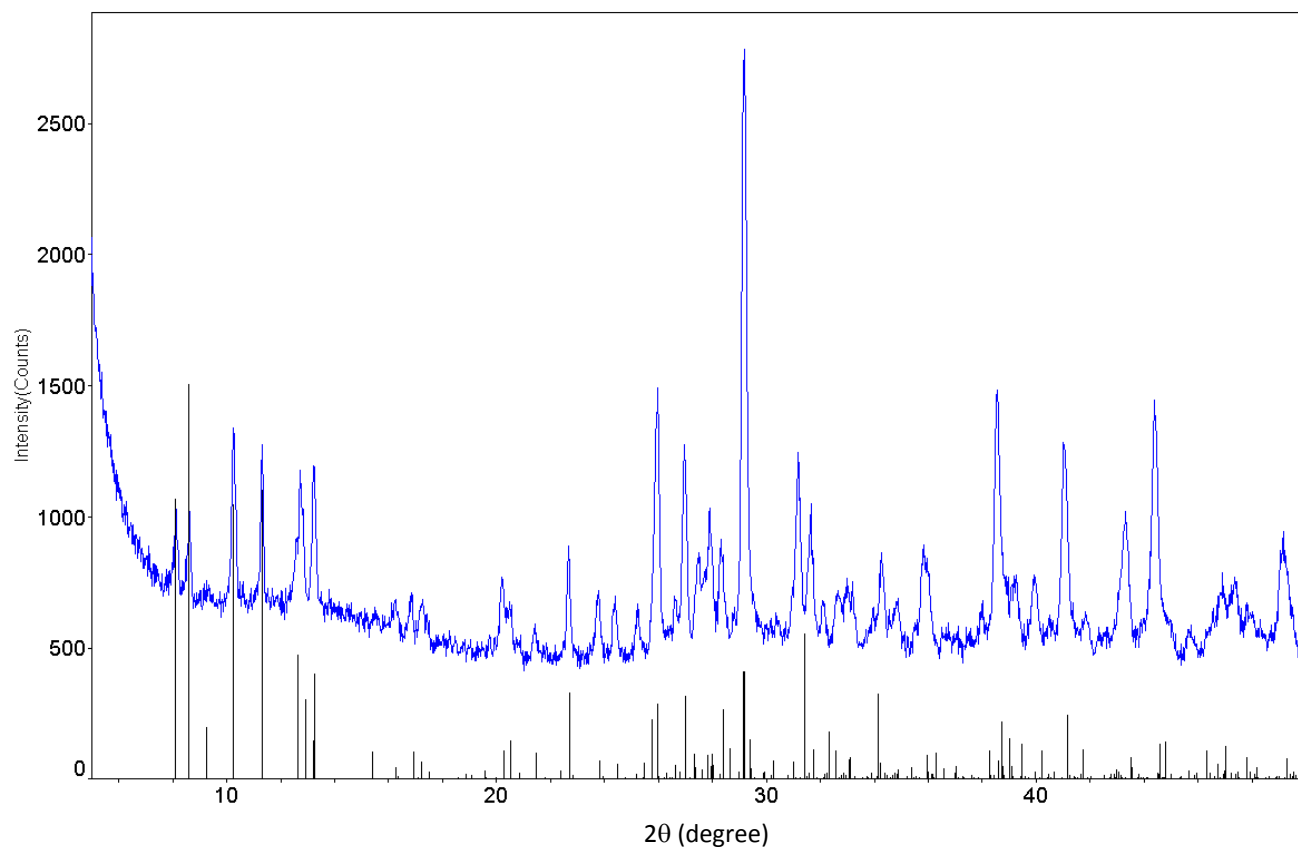
Fig.S4 UV-Vis spectra of **3** (solid line), crude product (dotted line) and $CrCl_3 \cdot 6H_2O$ (dashed line).

Figure S5. FT-IR spectra of (a) crude product (b) **2** (c) **3**. The dotted lines show the absorption band positions.

Figure S6. Powder XRD pattern of **3** (blue) and simulated pattern (black)

C) References

[1] M. R.Antonio, M. D. Nyman, T. M.Anderson, *Angew. Chem., Int. Ed.* 2009, **48**, 6136-6140.
[2] M. Valiev, E. J. Bylaska, N. Govind, K. Kowalski, T. P. Straatsma, H. J. J. van Dam, D. Wang, J. Nieplocha, E. Apra, T. L.Windus, W. A. de Jong, *Comput. Phys. Commun.* 2010, **181**, 1477–1489.
[3] M. J. Frisch *et al*, Gaussian 09 Revision A.1, Gaussian Inc. Wallingford CT 2009.
[4] M. K. Nazeeruddin, F. De Angelis, S. Fantacci, A. Selloni, G. Viscardi, P. Liska, S. Ito, B. Takeru, M. Grätzel, *J. Am. Chem. Soc.* 2005, **127**, 16835–16847.
[5] D. Ravelli, D. Dondi, M. Fagnoni, A. Albini, A. Bagno, *J. Comput. Chem.* 2011, **32**, 2983–2987.
[6] Bruker (2001). *SADABS.* Bruker AXS Inc., Madison, Wisconsin, USA.
[7] G. M. Sheldrick, *Acta Cryst.* 2008, A**64**, 112-122.